

Load-sharing ratio analysis of reinforced concrete filled tubular steel columns

Alifujiang Xiamuxi*^{1,2} and Akira Hasegawa¹

¹Department of Environmental and Civil Engineering, Hachinohe Institute of Technology, Hachinohe, Japan

²College of Architectural and Civil Engineering, Xinjiang University, Urumqi, China

(Received month October 24, 2011, Revised March 30, 2012, Accepted April 01, 2012)

Abstract. It was clear from the former researches on reinforced concrete filled tubular steel (RCFT) structures that RCFT structures have different performance than concrete filled steel tubular (CFT) structures. However, despite of that, load-sharing ratio of RCFT is evaluating by the formula and range of CFT given by JSCE. Therefore, the aim of this investigation is to study the load-sharing ratio of RCFT columns subjected to axial compressive load by performing numerical simulations of RCFT columns with the nonlinear finite element analysis (FEA) program - ADINA. To achieve this goal, firstly proper material constitutive models for concrete, steel tube and reinforcement are proposed. Then axial compression tests of concrete, RC, CFT, and RCFT columns are carried out to verify proposed material constitutive models. Finally, by the plenty of numerical analysis with small-sized and big-sized columns, load-sharing ratio of RCFT columns was studied, the evaluation formulas and range were proposed, application of the formula was demonstrated, and following conclusions were drawn: The FEA model introduced in this paper can be applied to nonlinear analysis of RCFT columns with reliable results; the load-sharing ratio evaluation formula and range of CFT should not be applied to RCFT; The lower limit for the range of load-sharing ratio of RCFT can be smaller than that of CFT; the proposed formulas for load-sharing ratio of RCFT have practical mean in design of RCFT columns.

Keywords: RCFT structures; CFT structures; load-sharing ratio; numerical simulation; constitutive model; evaluation formula.

1. Introduction

In the recent years, along with the enlargement of structures in the cities, the composite structures which have better bearing capacity and seismic performance are urgently expected, and also its applications are being promoted.

The composite structures obtained its excellent characteristic by combining the two kinds of materials which is totally different and has no so excellent characteristic singly.

(1) Taking merits of each material, the composite structures are neither only load-proof nor earthquake resistance, but also leads to an enormous reduction in the construction expense by possessing enough rigidity and deformation characteristic and shortening the construction time(or lowering construction cost).

(2) Because of its high strength, the cross-section of members of composite structures can be small in

* Corresponding author, Mr., E-mail: d10301@hi-tech.ac.jp

size and then slimming down of the whole structure, and so enable the construction of a building in more beautiful spectacle in the cities with the limited space.

In Hanshin-Awaji earthquake of Japan in 1995, the concrete filled steel tubular (CFT) structures were avoided from collapse while most of reinforced concrete (RC) and steel structures were heavily damaged due to shear failure and local buckling (JSCE 1999). As a reinforcement measure, steel plates were wrapped around the RC columns and RC was filled into the steel tubes. These reinforced structures can be considered as embryonic form of reinforced concrete filled tubular steel (RCFT) structures.

The brittle failure of CFT structures is concerned when it is considered to construct large-scaled structures and effective space (Wei *et al.* 2002, Xiao *et al.* 2005 and Xu *et al.* 2009), and then, RCFT structures which have high strength like CFT and can be adapted to large-scaled structures is developed and studied in the terms of practical utilization. Fig. 1 shows the model of CFT and RCFT.

Whatever CFT or RCFT, selection of steel tube is the first step of the designing process and the proper selection of thickness of steel tube is utmost important for overall performance and economical condition. This must be taken into serious consideration especially when construct large-scaled structures.

Load-sharing ratio is one of the important indexes to estimate thickness of steel tube for both CFT and RCFT which means strength ratio of steel tube to overall strength of CFT or RCFT. Currently, when design CFT and RCFT structures, load-sharing ratio is evaluated by same formula given by JSCE (1999).

RCFT is a composite structure which is aimed at improving the shear strength of CFT structure by inserting reinforcement, and the existence of reinforcement will change the mechanical properties of CFT. Some research results until now (Endo *et al.* 2000, Wang *et al.* 2002, Zhao 2003, Wei *et al.* 2005, Sato 2008, Han *et al.* 2010, and Miao 2010) proved that the bearing capacity, ductility, deformation and seismic performance of RCFT structures are increased compared with CFT. This means RCFT have different performance than CFT, and therefore it is not so appropriate using same evaluation method of load-sharing ratio for CFT and RCFT.

Therefore, the aim of this investigation is to study the load-sharing ratio of RCFT columns subjected to axial compressive loads by performing numerical simulations of RCFT columns with the nonlinear finite element analysis (FEA) program - ADINA. To achieve this goal, firstly proper material constitutive models for concrete, steel tube and reinforcement are proposed. Then axial compression

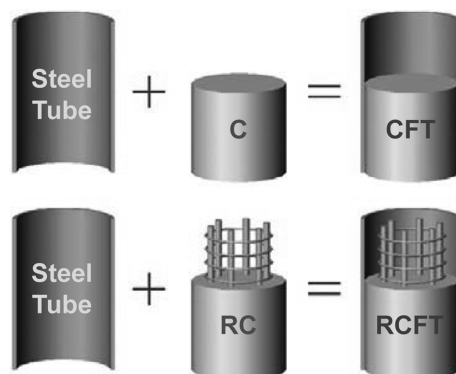


Fig. 1 Model of CFT and RCFT

tests of concrete, RC, CFT, and RCFT columns are carried out to verify proposed material constitutive models. Finally, by the plenty of numerical analysis, load-sharing ratio of RCFT columns are studied and discussed.

2. Definition of load-sharing ratio

According to JSCE (1999), load-sharing ratio of CFT (γ_c) column is defined by following equation

$$\gamma_c = \frac{P_s}{P_s + P_c} \quad (1)$$

where $P_s = \sigma_{cu0} \cdot A_s$ is bearing capacity of steel tube, $P_c = \sigma_c \cdot A_c$ bearing capacity of concrete, σ_{cu0} is axial compressive strength of steel tube without consideration of local buckling, A_s is cross-section area of steel tube, σ_c is strength of concrete (this value can be $\sigma_c = 0.85\sigma_k$ in design, where σ_k is norm value of load), A_c is cross-section area of concrete.

And the value of γ_c calculated by Eq. (1) should be in the following range

$$0.2 \leq \gamma_c \leq 0.9 \quad (2)$$

In general, if the value of γ_c too small, sharing load of concrete would be significant and CFT performs like concrete. If the value of γ_c is too big, sharing load of steel tube would be significant and steel tube is over performed without exerting assets of composite column.

Currently load-sharing ratio of RCFT columns is also calculated using these equations (Suzuki 2008, Sato 2008). In this study also, Eq. (1) is used to estimate the proper thickness of steel tube for the analysis at start.

3. Material properties and FEA model

3.1 Concrete

For concrete material modeling, concrete model built in ADINA is adopted. ADINA R&D Inc. (2008) describes the detailed information about formulation of concrete material.

According to ADINA R&D Inc. (2008), the characteristics of concrete model in ADINA are assumed compression crushing failure at high compression and tensile failure at a maximum principle tensile stress which is relatively small in comparison to compressive stress. Also, strain softening occurs from the compression crushing failure point to an ultimate strain point.

In ADINA, the general multi axial stress-strain relations are derived from uniaxial stress-strain relationship. As to multi axial stress-strain relations, ADINA provides three features, that is, a nonlinear stress-strain relation to allow the material weakening behavior after maximum stress, failure envelopes for tensile failure and compressive crushing, and concrete model for post-crushing and cracking.

As ADINA R&D Inc (2008) described, uniaxial stress-strain relationship used in this analysis for concrete material is shown as Fig. 2, where σ_c is maximum uniaxial compressive stress, ε_c is uniaxial strain corresponding to σ_c , σ_u is ultimate uniaxial compressive stress, ε_u is ultimate uniaxial compressive strain corresponding to σ_u , σ_t is uniaxial cut-off tensile strength; σ_{tp} is post-cracking uniaxial cut-off

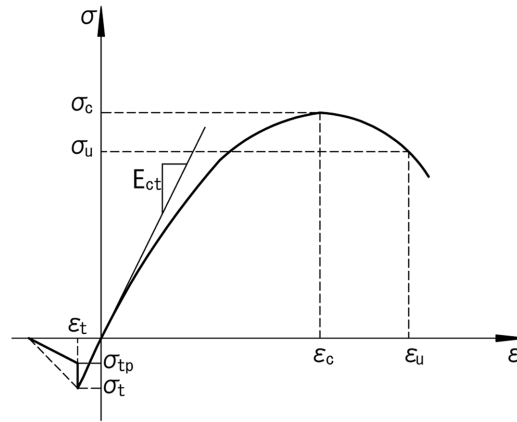


Fig. 2 Equivalent uniaxial stress-strain curve for concrete

tensile strength(if $\sigma_{tp} = 0$, ADINA sets $\sigma_{tp} = \sigma_t$, shown as oblique dotted line in Fig. 2, ε_t is uniaxial strain corresponding to σ_t , E_{ct} uniaxial tangent modulus at zero strain (must be greater than σ_c/ε_c).

In addition, for strain states beyond ε_u in compression, ADINA assumes that stresses are linearly released to zero, using the following modulus

$$E_u = \frac{\sigma_u - \sigma_c}{\varepsilon_u - \varepsilon_c} \quad (3)$$

And thus, confined concrete can be modeled using close values for σ_u and σ_c (ADINA R&D Inc. 2008).

Since most characteristic properties of RCFT is similar to CFT, Some research (Hu *et al.* 2003, Lakshmi *et al.* 2002, Wu *et al.* 2000, Jiang *et al.* 2007, and Choi *et al.* 2010) results on numerical analysis of CFT can be adopted to RCFT.

When concrete is subjected to laterally confining pressure, the uniaxial compressive strength σ_c and the corresponding strain ε_c are much higher than those of unconfined concrete. σ_c and ε_c can be estimated by the following equations (Mander *et al.* 1988)

$$\sigma_c = \sigma_{c0} + k_1 \sigma_l \quad (4)$$

$$\varepsilon_c = \varepsilon_{c0} \left(1 + k_2 \frac{\sigma_l}{\sigma_{c0}} \right) \quad (5)$$

Where σ_l represents the confining pressure around the concrete core; σ_{c0} is maximum uniaxial compressive stress of unconfined concrete; ε_{c0} is uniaxial strain of unconfined concrete corresponding to σ_{c0} ; the k_1 and k_2 are constants and can be obtained from experimental data. Meanwhile, the constants k_1 and k_2 were set as 4.1 and 20.5 based on the studies of Richart *et al.* (1928).

σ_l can be estimated using the following equations proposed by Hu *et al.* (2003)

$$\frac{\sigma_l}{f_{sy}} = 0.044 - 0.000832 \frac{D}{t} \quad \left(21.7 \leq \frac{D}{t} \leq 47 \right) \quad (6a)$$

$$\frac{\sigma_l}{f_{sy}} = 0.0062 - 0.0000357 \frac{D}{t} \quad \left(47 \leq \frac{D}{t} \leq 150 \right) \quad (6b)$$

Where f_{sy} is yield strength of steel tube; D is outer diameter of steel tube; t is thickness of steel tube.

The value of σ_{c0} is determined by material test or material property and corresponding value of ε_{c0} is usually around the range of 0.002 to 0.003, a representative value suggested by ACI Committee 318 (1999) and used in the analysis is $\varepsilon_{c0} = 0.003$.

According to Hu *et al.* (2003), the value of σ_u can be determined by $\sigma_u = k_3 \sigma_c$ and the value of ε_u can be ranged in $1.2\varepsilon_c \leq \varepsilon_u \leq 11\varepsilon_c$ (Hu *et al.* 2003, Endo *et al.* 2005, Nishida *et al.* 2007, lower limit for unconfined concrete, upper limit for confined concrete). The k_3 is defined as material degradation parameter. k_3 can be estimated for confined concrete using the following equations proposed by Hu *et al.* (2003)

$$k_3 = 1 \quad \left(21.7 \leq \frac{D}{t} \leq 40 \right) \quad (7a)$$

$$k_3 = 0.0000339 \left(\frac{D}{t} \right)^2 - 0.010085 \frac{D}{t} + 1.35 \quad \left(40 \leq \frac{D}{t} \leq 150 \right) \quad (7b)$$

In addition, Tadahiko *et al.* (2001) used the value of $k_3 = 0.8$ for RC in ADINA.

The value of $\sigma_t = 0.23(\sigma_c)^{2/3}$ according to JSCE (1999), the value of σ_{tp} can be zero according to ADINA R&D Inc. (2008), and the value of ε_t is calculated automatically using $\varepsilon_t = \sigma_t / E_{ct}$ in ADINA.

The initial modulus of elasticity of concrete E_{ct} is highly correlated to its compressive strength and can be calculated with reasonable accuracy from the empirical equation (ACI 1999)

$$E_{ct} = 4700 \sqrt{\sigma_c} \quad (8)$$

The Poisson's ratio ν_c of concrete under uniaxial compressive stress ranges from 0.15 to 0.22, with a representative value of 0.19 or 0.20 (ASCE 1982). In this study, the Poisson's ratio of concrete is assumed to be $\nu_c = 0.2$.

In addition, some input parameters to represent the multi axial compressive behavior of concrete are selected from the default values of concrete material model in ADINA, and triaxial failure curve is taken as Kuper model. And two critical strain constants, which are scalar parameters to calculate uniaxial compressive failure and ultimate strain values, are selected as 1.4 and -0.4 respectively.

3.2 Steel tube and reinforcement

Bilinear elastic-perfectly plastic material model built in ADINA is used for steel tube and reinforcement modeling. And this material assumes the Von Mises yield condition and an associated flow rule by the Von Mises yield function in ADINA program. This model also allows an isotropic and kinematic hardening rule, and the isotropic hardening rule is selected for this analysis.

Constitutive law for this model is shown as Fig. 3, where σ_y is yield stress, ε_y is yield strain, σ_p is ultimate strength; ε_p is strain corresponding to σ_p , E_s is Young's modulus, E_{st} is strain hardening modulus.

Poisson's ratio ν_s and Young's modulus E_s are set to $\nu_s = 0.3$ and $E_s = 2.0 \times 10^5$ N/mm² respectively. According to JSCE (2008), E_{st} can be assumed $E_{st} = (0.01 \sim 0.0125)E_s$. Other parameters can be determined by material testing or material property.

In addition, ADINA R&D Inc. (2008) describes the detailed information about formulation of bilinear material.

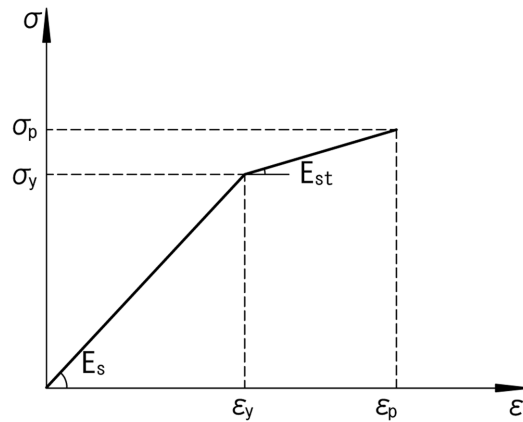


Fig. 3 Constitutive law for steel

3.3 FEA modeling

As to the contacts between steel tube and concrete, Jiang (2007) analyzed CFT columns in ADINA with following assumptions: 1) steel tube and concrete is completely bonded; 2) steel tube and concrete contacted without friction; 3) steel tube and concrete contacted with friction. And concluded that frictionless contact is more applicable while simulate the contacts between steel tube and concrete. Choi *et al.* (2010) also adopted frictionless contact for modeling contacts between steel tube and concrete in ADINA, and achieved applicable results. Therefore, in this analysis, frictionless constrained contact model built in ADINA (ADINA R&D Inc. 2008) is employed for the contacts between steel tube and RC.

To achieve more accurate FEA results and comparable failure shape against experiment, the columns modeled entirely (not utilizing symmetrical characteristics) and calculations are carried out in 100 load steps. The displacement is used for both loading method and convergence criteria.

The bottom surface of column is fixed without deformation in all directions, and the load is applied in terms of displacement through a steel cap which is placed on the top surface of column and fixed without horizontal displacement but allowing rotations and axial displacements.

In the FEA mesh, both the concrete and the steel tube are modeled by 10-node 3-D solid elements (three degrees of freedom per node). The reinforcements are modeled by two-node truss elements. Through many trial and error procedures, element edge length is select as 15 mm for mesh densities.

To improve convergence of FEA, the following techniques are used: 1) applying incompatible element mode in concrete can improve accuracy, but convergence will become worth, therefore compatible element mode in concrete is used; 2) higher numerical integration order (4-6) for concrete is selected, although there is some speed penalties; 3) The convergence tolerance is set to 0.05; 4) Equation solver is selected as sparse matrix algorithm, iteration method is selected as full Newton method, and number of iterations are set to 45; 5) Automatic time stepping (ATS) method with low speed dynamic model damping is applied.

4. Validation of FEA model

4.1 Outline of the compression test and FEA model

To validate the reliability of FEA Model, axial compression tests of concrete, RC, CFT and RCFT columns were carried out.

The outer diameter and height of all specimens was $D = 150$ mm and $H = 450$ mm. Material of steel tube was SS400 (Japanese Industrial Standard: JIS), yield strength was $f_{sy} = 304$ N/mm², and thickness was $t = 1.2$ mm. Material of axial reinforcement was SD295 (JIS), yield strength was $f_{sa} = 295$ N/mm², and number was 6, diameter was $d_{sa} = 6$ mm. Material of stirrups was SS400 (JIS), yield strength was $f_{sl} = 304$ N/mm², spacing was 30 mm, diameter was $d_{sl} = 3$ mm. Diameter of core RC was $d_c = 147.6$ mm (150 mm for RC) and cover thickness of reinforcement was $a_s = 43.8$ mm (45 mm for RC). And strength of concrete from uniaxial compression test was $\sigma_{c0} = 40$ N/mm².

Specimens were divided into 4 groups with corresponding labels (concrete, RC, CFT, and RCFT) and 3 same specimens were prepared for each group. The more detailed information about the specimens is shown in the Table 1 and Fig. 4.

The items measured from the experiment were load, axial deformation and strains. 4 deformation transducers were installed on the top of specimens to measure axial deformation. Strains of steel tube were measured by 8 strain gauges placed circumferentially and longitudinally at the outside longitudinal

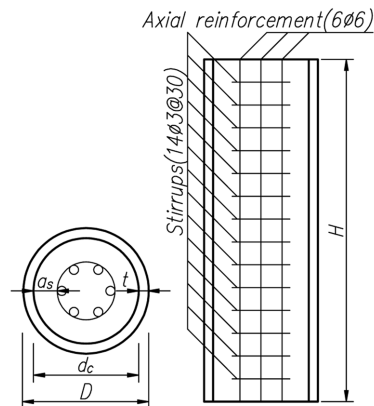


Fig. 4 Cross-section and reinforcement

Table 1 Outline of the specimens

Group name	Concrete	RC	CFT	RCFT
Specimen label	C-T-(1,2,3)	RC-T-(1,2,3)	RCFT-T-(1,2,3)	RCFT-T-(1,2,3)
Steel tube	-	-	SS400, $t = 1.2$ mm	SS400, $t = 1.2$ mm
Axial reinforcement	-	SD295, Number 6, $d_{sa} = 6.0$ mm	-	SD295, Number 6, $d_{sa} = 6.0$ mm
Stirrups	-	SS400, spacing 30 mm, $d_{sl} = 3.0$ mm	-	SS400, spacing 30 mm, $d_{sl} = 3.0$ mm
Ratio of axial reinforcement	-	1.08%	-	1.11%



Fig. 5 Installation of specimen

Table 2 Parameters used in the FEA modeling

Parameters Labels	D (mm)	t (mm)	d_c (mm)	D/t	σ_l (N/ mm ²)	k_3	σ_c (N/ mm ²)	ε_c (m/m)	σ_{lt} (N/ mm ²)	ε_{lt} (m/m)	σ_t (N/ mm ²)	E_{ct} (N/mm ²)
C-A	150.0	-	150.00	-	0	0.60	40.00	0.0030	24.00	0.0036	2.69	2.973×10^4
RC-A	150.0	-	150.00	-	0	0.60	40.00	0.0030	24.00	0.0090	2.69	2.973×10^4
CFT-120	150.0	1.20	147.60	125.00	0.53	0.62	42.17	0.0038	26.10	0.0419	2.79	3.052×10^4
RCFT-120	150.0	1.20	147.60	125.00	0.53	0.62	42.17	0.0038	26.10	0.0419	2.79	3.052×10^4

Table 3 Maximum (Max.) load and displacement (Disp.)

Labels for Test	Labels for FEA	Max. load (kN)		Average Max. load of test (kN)	Disp. (mm)		Average Disp. of test (mm)
		Test	FEA		Test	FEA	
RCFT-T-1	RCFT-120	817.5	871.48	816.0 (Error: 6.37%)	2.55	2.10	2.29 (Error: -9.05%)
RCFT-T-2		821.4			2.03		
RCFT-T-3		809.0			2.29		
CFT-T-1	CFT-120	868.5	900.00	843.6 (Error: 6.27%)	2.04	2.09	2.12 (Error: -1.44%)
CFT-T-2		821.4			2.20		
CFT-T-3		841.0			2.13		
RC-T-1	RC-A	640.3	698.60	640.95 (Error: 8.25%)	1.38	1.50	1.39 (Error: 7.33%)
RC-T-2		*414.6			*3.55		
RC-T-3		641.6			1.40		
C-T-1	C-A	619.3	691.05	621.7 (Error: 10.00%)	1.28	1.30	1.32 (Error: -1.54%)
C-T-2		568.3			1.34		
C-T-3		677.5			1.34		

* The numbers marked with “*” mean the results are abnormal and not used in the analysis.

center of specimens. Only 2 strain gauges were placed symmetrically for 2 of 6 axial reinforcements at the longitudinal center. To measure the compressive strain of the concrete, a mold strain gauge was

placed inside of the concrete at longitudinal center. Fig. 5 shows the installation of specimens.

The material parameters used in the FEA model are laid out in the Table 2. In addition, for all model: $f_{sy} = 304 \text{ N/mm}^2$, $f_{sa} = 295 \text{ N/mm}^2$, $f_{st} = 304 \text{ N/mm}^2$, $\sigma_{c0} = 40 \text{ N/mm}^2$, and $H = 450 \text{ mm}$.

4.2 Results and discussion

The results of FEA and experiment are given in Table 3 and the curves of axial force versus axial displacement for these columns are plotted against the experimental data in Fig. 6.

Load-displacement curves in Fig. 6 tell that FEA results of CFT, RC and concrete columns are in very good agreement with experimental results. FEA results of RCFT although are in good agreement with experimental results, but there is a little difference especially after the maximum load. This may be because the confinement rule of CFT in Sec. 3 is applied to RCFT and neglected the confinement effect of reinforcement in core RC.

FEA-to-test errors of maximum load and corresponding displacements in Table 3 are all in the acceptable range (all under 10%). And also the failure shapes of test and FEA in Fig. 7 are very alike

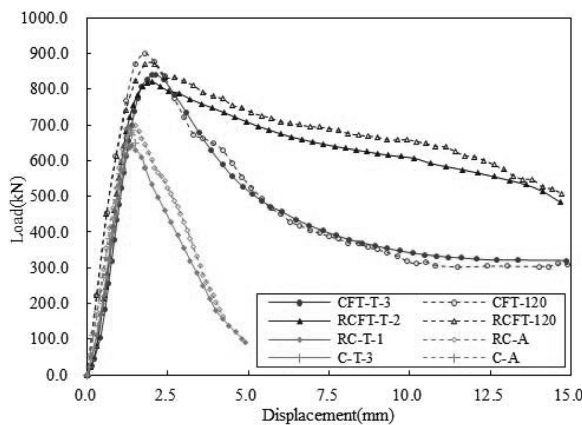


Fig. 6 Comparison of load-displacement curves

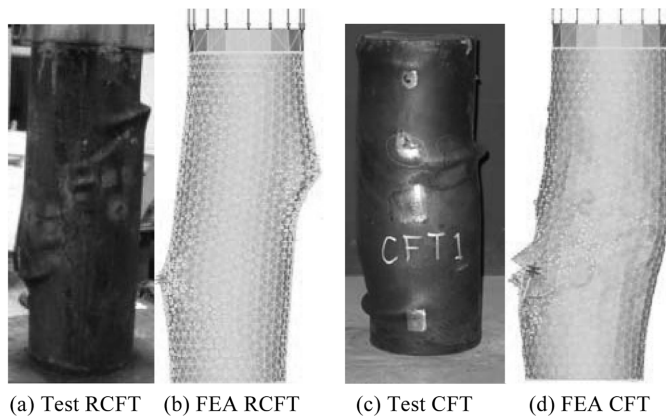


Fig. 7 Comparison of failure shapes

each other.

In conclusion, FEA model in Sec. 3 is reliable, can be applied to the numerical analysis of RCFT with ADINA.

5. Load-sharing ratio analysis of RCFT columns

5.1 Parameters for FEA modeling

Same column size and materials as former section are used in FEA modeling.

The only changing parameter is thickness (t) of steel tube, and relevantly the value of γ_c , a_s and d_c will be changing along with t . And the steel tubes assumed to be made from steel plates provided in JIS by welding. Appropriate values for t are selected basing upon the calculation results of γ_c by Eq. (1). And then, 16 RCFT plus 1 CFT total 17 column models are determined. The cross-section and arrangement of reinforcement in core RC are shown in Fig. 4, and the Table 4 shows the essential parameters used in ADINA while FEA modeling.

5.2 FEA results and discussion

The results of FEA are given in Table 5 and the curves of axial load versus axial displacement for these columns are plotted in Fig. 8 and Fig. 9. In Table 5, P_u is bearing capacity of the RCFT column, P_r is bearing capacity of reinforcement, γ_p is actual load-sharing ratio by FEA, γ_c is load-sharing ratio by Eq. (1).

Table 4 Parameters used in FEA modeling

Parameters Labels	D (mm)	t (mm)	d_c (mm)	D/t	σ_l (N/ mm ²)	k_3	σ_c (N/ mm ²)	ε_c (m/m)	σ_u (N/ mm ²)	ε_u (m/m)	σ_l (N/ mm ²)	E_{ct} (N/mm ²)	D (mm)
CFT-2400	150.0	24.00	102.00	0.898	6.3	7.89	1.00	72.34	0.0151	72.34	0.1664	3.99	3.997×10 ⁴
RCFT-040	150.0	0.40	149.20	0.076	375.0	0.26	0.60	41.05	0.0034	24.63	0.0373	2.74	3.011×10 ⁴
RCFT-050	150.0	0.50	149.00	0.093	300.0	0.26	0.60	41.05	0.0034	24.63	0.0373	2.74	3.011×10 ⁴
RCFT-055	150.0	0.55	148.90	0.101	272.7	0.26	0.60	41.05	0.0034	24.63	0.0373	2.74	3.011×10 ⁴
RCFT-060	150.0	0.60	148.80	0.110	250.0	0.26	0.60	41.05	0.0034	24.63	0.0373	2.74	3.011×10 ⁴
RCFT-070	150.0	0.70	148.60	0.126	214.3	0.26	0.60	41.05	0.0034	24.63	0.0373	2.74	3.011×10 ⁴
RCFT-080	150.0	0.80	148.40	0.141	187.5	0.26	0.60	41.05	0.0034	24.63	0.0373	2.74	3.011×10 ⁴
RCFT-120	150.0	1.20	147.60	0.199	125.0	0.53	0.62	42.17	0.0038	26.10	0.0419	2.79	3.052×10 ⁴
RCFT-230	150.0	2.30	145.40	0.328	65.2	1.18	0.84	44.83	0.0048	37.50	0.0529	2.90	3.147×10 ⁴
RCFT-300	150.0	3.00	144.00	0.393	50.0	1.34	0.93	45.50	0.0051	42.34	0.0557	2.93	3.170×10 ⁴
RCFT-450	150.0	4.50	141.00	0.500	33.3	4.95	1.00	60.27	0.0106	60.27	0.1166	3.54	3.649×10 ⁴
RCFT-650	150.0	6.50	137.00	0.602	23.1	7.54	1.00	70.91	0.0146	70.91	0.1605	3.94	3.958×10 ⁴
RCFT-1100	150.0	11.00	128.00	0.739	13.6	7.89	1.00	72.34	0.0151	72.34	0.1664	3.99	3.997×10 ⁴
RCFT-1400	150.0	14.00	122.00	0.795	10.7	7.89	1.00	72.34	0.0151	72.34	0.1664	3.99	3.997×10 ⁴
RCFT-2400	150.0	24.00	102.00	0.898	6.3	7.89	1.00	72.34	0.0151	72.34	0.1664	3.99	3.997×10 ⁴
RCFT-2858	150.0	28.58	92.84	0.924	5.2	7.89	1.00	72.34	0.0151	72.34	0.1664	3.99	3.997×10 ⁴
RCFT-3800	150.00	38.00	74.00	0.959	3.9	7.89	1.00	72.34	0.0151	72.34	0.1664	3.99	3.997×10 ⁴

Table 5 Results of FEA

Labels	D/t	Bearing capacity(kN)				γ_p	γ_c	Toughness ($\times 10^3 \text{J/m}^3$)
		P_s	P_c	P_r	P_u			
C-A	-	-	691.05	-	691.05	-	-	0.6
RC-A	-	-	648.24	50.37	698.60	-	-	1.8
CFT-120	125.0	207.05	692.95	-	900.00	0.230	0.199	6.7
CFT-2400	6.3	3940.16	493.90	-	4434.05	0.889	0.898	96.4
RCFT-040	375.0	14.48	678.48	50.72	743.68	0.019	0.076	2.8
RCFT-050	300.0	162.67	568.51	50.71	781.88	0.208	0.093	4.1
RCFT-055	272.7	164.36	572.19	50.71	787.27	0.209	0.101	7.2
RCFT-060	250.0	176.80	558.85	50.72	786.37	0.225	0.110	7.7
RCFT-070	214.3	190.88	556.51	50.71	798.10	0.239	0.126	8.1
RCFT-080	187.5	201.03	557.19	50.70	808.93	0.249	0.141	8.3
RCFT-120	125.0	222.62	598.13	50.73	871.48	0.255	0.199	9.8
RCFT-230	65.2	321.30	671.49	50.88	1043.67	0.308	0.328	20.8
RCFT-300	50.0	404.66	674.13	50.87	1129.66	0.358	0.393	25.0
RCFT-450	33.3	827.08	883.77	52.03	1762.89	0.469	0.500	46.9
RCFT-650	23.1	1222.30	965.80	52.52	2240.61	0.546	0.602	59.8
RCFT-1100	13.6	2075.08	913.80	51.47	3040.35	0.683	0.739	78.6
RCFT-1400	10.7	2625.56	797.15	52.75	3475.46	0.755	0.795	89.4
RCFT-2400	6.3	4317.53	513.25	52.82	4883.61	0.884	0.898	122.8
RCFT-2858	5.2	4842.79	550.21	53.09	5446.10	0.889	0.924	136.2
RCFT-3800	3.9	6121.26	295.61	52.53	6469.40	0.946	0.959	160.1

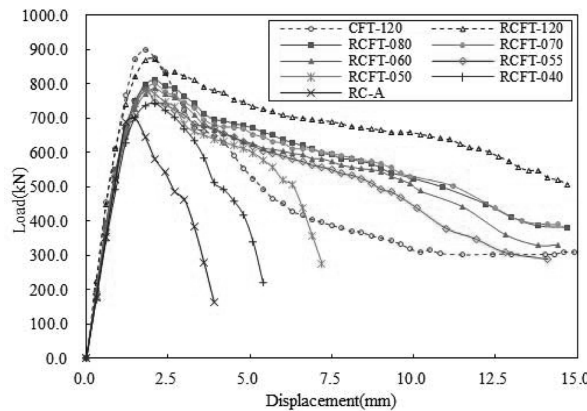


Fig. 8 Load-displacement curves ($\gamma_c = 0.08\sim 0.20$)

5.2.1 Range for load-sharing ratio of RCFT

Toughness is property of a material that enables it to absorb and distribute within itself relatively large amounts of energy (both stresses and strains) of repeated impacts and/or shocks, and undergo considerable deformation before fracturing or failing. Toughness can be determined by measuring the

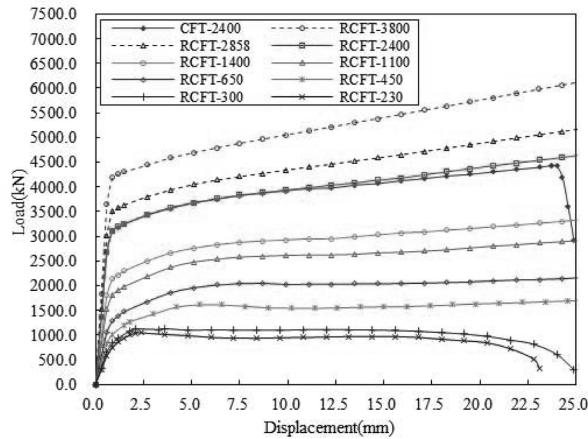


Fig. 9 Load-displacement curves ($\gamma_c = 0.33\sim 0.96$)

area (i.e., by taking the integral) underneath the stress-strain curve. It's energy of mechanical deformation per unit volume prior to fracture. It is one of the important indexes to evaluate anti-seismic capacity of the structure.

In this study, toughness of the columns is determined by calculating the envelope area of load-displacement curves shown as Fig. 8 and Fig. 9, and was made as one of the indexes to determine the range for load-sharing ratio of RCFT (γ_s).

Meanwhile, range of γ_s can be determined referring to the range of γ_c ($0.2 \leq \gamma_c \leq 0.9$).

(1) Lower limit

In Table 5, γ_c of CFT-120 is $\gamma_c = 0.2$ (corresponding to lower limit), corresponding value of toughness is 6.7, and minimum value of toughness for RCFT which is greater than 6.7 is 7.2.

In Fig. 8, before RCFT-055, the curves of RCFT are above to the CFT-120. After the RCFT-055, the curves of RCFT are below to the CFT-120, and the curve shapes are approaching to that of RC. This means that if the value of γ_s too small, sharing load of RC would be significant and RCFT performs like RC.

Therefore, It can be determined that the lower limit of γ_s can be 0.10 for RCFT which is corresponding to RCFT-055 in Table 5.

This conclusion tells that RCFT can use thinner steel tube without decrease of performance. From the viewpoint of construction cost, this will have actual mean while constructing large-scaled structures with RCFT.

(2) Upper limit

In Table 5, γ_c of CFT-2400 is $\gamma_c = 0.9$ (corresponding to upper limit), corresponding value of toughness is 96.4, and minimum value of toughness for RCFT which is greater than 96.4 is 122.8.

In Fig. 9, the curve of CFT-2400 is comparable only with the curve of RCFT-2400.

Therefore, It can be determined that the upper limit of γ_s can be 0.90 for RCFT which is corresponding to RCFT-2400 in Table 5.

In addition, according to Fig. 10, RCFT-2400 is under healthy condition and ready for further loading while CFT-2400 begin to failure. This indicates that the RCFT has better performance than CFT even with higher load-sharing ratio. Again, according to Fig. 9, above the RCFT-2400, the shape of curves are approaching to the shape of bilinear constitutive curve of steel tube, this means that if the value of γ_s is too big, sharing load of steel tube would be significant and steel tube is over performed without

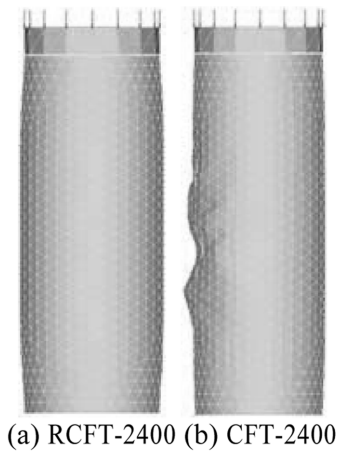


Fig. 10 Ultimate status

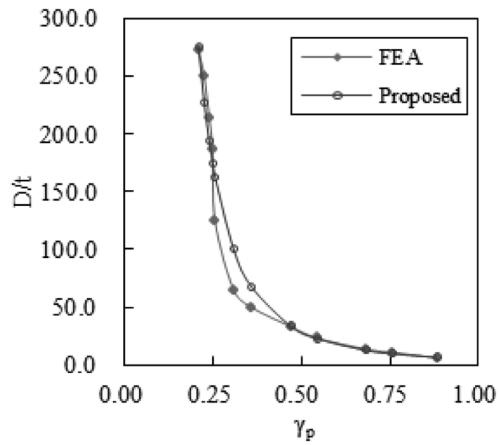


Fig. 11 D/t versus γ_p

exerting assets of composite column.

5.2.2 Further discussion on big-sized columns

The conclusions above are obtained through the results of small sized experimental columns, to ensure the reliability of the conclusions when they are applied to design of actual constructions, analysis of some big-sized columns paired with some key columns in Table 5 (CFT-120, CFT-2400, RCFT-55, RCFT-120 and RCFT-2400) were carried out. The size of big-sized columns were determined by magnifying the size of 150×450 mm to 1000×3000 mm(magnification factor is 6.6667), correspondingly the labels are changed to CF-120, CF-2400, RF-55, RF-120 and RF-2400. And FEA or other parameters were kept as same as small-sized ones.

The results of FEA are given in Table 6, Fig. 12 and Fig. 13.

From the results, in case of the conclusions on range of γ_s , comparisons between small-sized and big-sized columns can be described as follows:

(1) Difference of toughness between CFT-120 (6.7) and RCFT-55(7.2) is $\Delta_1 = 7.5\%$, difference of toughness between CF-120 (1817.0) and RF-55 (1958.2) is $\Delta_2 = 7.8\%$, and thus difference between Δ_1 and Δ_2 is 4.0%;

(2) Difference of toughness between CFT-2400 (96.4) and RCFT-2400 (122.8) is $\Delta_1 = 27.4\%$, difference of toughness between CF-2400 (25362.8) and RF-2400 (31916.1) is $\Delta_2 = 25.8\%$, and thus difference between Δ_1 and Δ_2 is 5.8%;

Table 6 FEA results of big-sized columns

Labels	D/t	Bearing capacity (kN)				γ_p	γ_c	Toughness ($\times 10^3 J/m^3$)
		P_s	P_c	P_r	P_u			
CF-120	125.00	8991.80	30507.50	-	39499.30	0.228	0.199	1817.0
CF-2400	6.25	171727.60	23065.40	-	194793.00	0.882	0.898	25362.8
RF-55	272.73	7210.11	25063.40	2426.49	34700.00	0.208	0.101	1958.2
RF-120	125.00	9982.50	26571.10	2427.30	38980.90	0.256	0.199	2616.6
RF-2400	6.25	184530.04	21909.80	2545.16	208985.00	0.883	0.898	31916.1

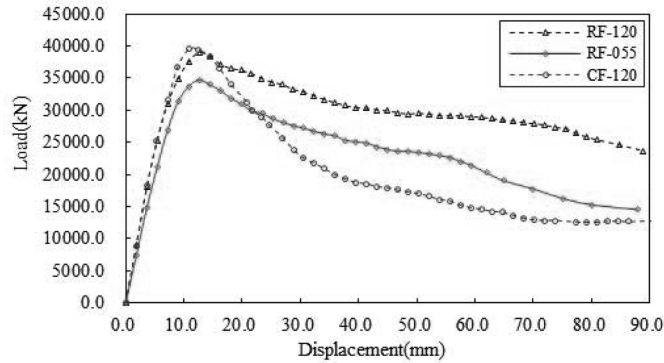


Fig. 12 Load-displacement curves of big-sized columns (1)

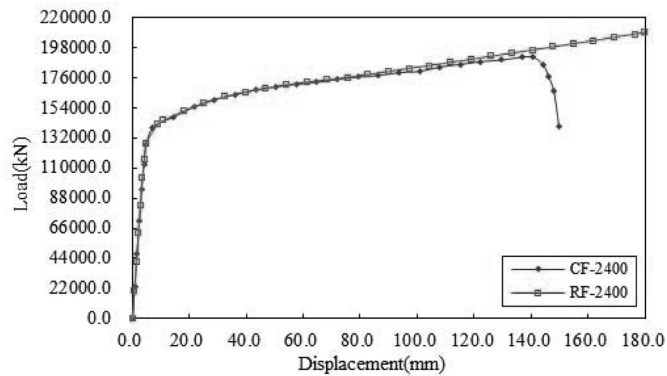


Fig. 13 Load-displacement curves of big-sized columns (2)

(3) It is clear from the Fig. 12 and Fig. 13 that the curve shapes of big-sized columns (CF-120, CF-2400, RF-55, RF-120 and RF-2400) are completely same with that of their small-sized pairs (CFT-120, CFT-2400, RCFT-55, RCFT-120 and RCFT-2400);

(4) The values of Δ_p in Table 5 and Table 6 are also very close with each other.

These comparisons may tell that the results of big-sized columns are same with the results of small-sized ones, and the same conclusions about range of γ_s can be drawn.

5.2.3 Evaluation equation for load-sharing ratio of RCFT

(1) Empirical equation for D/t versus γ_p

In the Table 5, corresponding to range of γ_s ($0.1 \leq \gamma_s \leq 0.9$) determined in previous section, range of γ_p may be $0.21 \leq \gamma_p \leq 0.88$. And thus, the values of D/t versus γ_p are drawn in Fig. 11. From the results, the following empirical equation may be proposed

$$\frac{D}{t} = \frac{4.7}{(\gamma_p)^{2.6}} \quad (0.21 \leq \gamma_p \leq 0.88) \quad (9)$$

(2) Evaluation equation for γ_s

According to scope of axial reinforcement ratio for RC columns in JSCE (2007), the γ_s value of

Table 7 Reinforcement ratio and load-sharing ratio

ρ (%)	0.80	1.30	1.80	2.30	2.80	3.30	3.80	4.30	4.80	5.30	5.80	6.00
γ_c	0.199											
γ_s	0.190	0.185	0.180	0.176	0.171	0.167	0.163	0.159	0.155	0.152	0.149	0.147
$(\gamma_c - \gamma_s)/\gamma_c$ (%)	4.51	7.13	9.61	11.96	14.19	16.31	18.32	20.25	22.08	23.83	25.51	26.16

RCFT-120 is calculated using Eq. (1) with consideration of reinforcement, and the results are listed in Table 7. In the table, ρ is axial reinforcement ratio, γ_c is load-sharing ratio calculated by Eq. (1) without consideration of reinforcement, γ_s is load-sharing ratio calculated by Eq. (1) with consideration of reinforcement.

It is clear from the Table 7 that there are significant differences between γ_s and γ_c especially with higher ρ , and differences between γ_s and γ_c are increasing linearly along with the increase of ρ . This means evaluation of γ for RCFT by Eq. (1) without consideration of reinforcement (using method for RCFT until now) is not correct.

Therefore, considering the strength value of axial reinforcement, the evaluation formula of load-sharing ratio for RCFT may be proposed as follows

$$\gamma_s = \frac{P_{ss}}{P_{ss} + P_{sa} + P_{sc}} \quad (10)$$

where $P_{ss} = \sigma_{cuo} \cdot A_{ss}$ is bearing capacity of steel tube, $P_{sa} = \sigma_{sa} \cdot A_{sa}$ is bearing capacity of axial reinforcement, $P_{sc} = \sigma_c \cdot A_c$ is bearing capacity of concrete, σ_{cuo} is axial compressive strength of steel tube without consideration of local buckling, A_{ss} is cross-section area of steel tube, σ_{sa} is axial compressive strength of axial reinforcement without consideration of local buckling, A_{sa} is total cross-section area of axial reinforcement, σ_c is strength of concrete (this value can be $\sigma_c = 0.85\sigma_k$ in design, where σ_k is norm value of strength), A_c is cross-section area of concrete.

According to previous section, the value of γ_s calculated by Eq. (10) should be in the following range

$$0.1 \leq \gamma_s \leq 0.9 \quad (11)$$

5.2.4 Application demo

Problem: A major column of a high building is assumed to use RCFT structure, and desired diameter of the column is $D = 1016$ mm, steel tube and reinforcement use SS400 ($f_{sy} = f_{sa} = 380$ N/mm²), reinforcement is 16 Φ 32 ($A_{sa} = 12707.2$ mm²), concrete uses $\sigma_c = 50$ N/mm². Try to select the thickness of steel tube.

Solution:

Assume load-sharing ratio within $0.21 \leq \gamma_p \leq 0.88$ as $\gamma_p = 0.40$

$$\frac{D}{t} = \frac{4.7}{(\gamma_p)^{2.6}} = \frac{4.7}{0.40^{2.6}} = 50.9$$

$$t = \frac{1016}{50.9} = 20.0 \text{ mm}$$

Hence, according to JIS, thickness of steel tube can be select as $t = 22$ mm.

$$\gamma_s = \frac{P_{ss}}{P_{ss} + P_{sa} + P_{sc}} = \frac{74506.0 \times 380}{74506.0 \times 380 + 12707.2 \times 380 + 875825.8 \times 50} = 0.36$$

$$0.1 \leq \gamma_s = 0.36 \leq 0.9$$

Hence, $t = 22$ mm is suitable for this RCFT column.

6. Conclusions

From the study results above, conclusions can be drawn as follows:

(1) The FEA model introduced in this paper, in cooperation with ADINA software, can be applied to nonlinear analysis of RCFT columns with reliable results.

(2) Load-sharing ratio of RCFT is differing from that of CFT, therefore, the load-sharing ratio evaluation formula and range of CFT should not be applied to RCFT. RCFT can use different formulas and range proposed in this paper to evaluate its load-sharing ratio.

(3) The lower limit for the range of load-sharing ratio of RCFT can be smaller than that of CFT. This means, compared with CFT, RCFT can use thinner steel tube without decrease of performance. From the viewpoint of construction cost, this will have actual mean while constructing large-scaled structures with RCFT.

(4) The upper limit for the range of load-sharing ratio of RCFT can be same with CFT, but RCFT possesses more toughness and bearing capacity than CFT.

(5) The Eq. (9) is a new formula which was not ever provided in JSCE standards, the demonstration of usage of the formula shows that it is simple and useful in design of RCFT columns.

(6) Some columns whose size is close to actual construction are analyzed and close or same results with small-sized experimental columns are obtained, and further ensured the reliability of the conclusions.

Meanwhile, in this study, confinement rule of CFT is used in FEA modeling of RCFT. Because of the existence of reinforcement, confinement rule of RCFT may differ from that of CFT. Therefore the circumferential binding and confinement effect of steel tube is worth being studied to further clarify the mechanical characteristics and mechanism of RCFT structures.

Acknowledgements

The experiments conducted in this study were made possible at the Structural Laboratory at the Hachinohe Institute of Technology, Hachinohe Japan. The authors will appreciate to staffs of the Laboratory. Mr. Suzuki Takuya (Kosaka technical research Co.Ltd.) provided us experimental papers, guidance and advices. Emeritus professor Shioi Yukitake listened to our problems and questions and provided sound advices. Supplemental cooperation and help were also provided by the students of Hasegawa laboratory. The authors thank all of them mentioned above.

References

ACI (1999), "Building code requirements for structural concrete and commentary", *American Concrete Institute*,

- ACI 318-99, Detroit.
- ASCE (1982), "ASCE task committee on concrete and masonry structure, state of the art report on finite element analysis of reinforced concrete", *ASCE*, New York.
- ADINA R&D Inc. (2008), "ADINA theory and modeling guide", *Report ARD08-7*, February.
- Choi, K.K. and Yan, X. (2010). "Analytical model of circular CFRP confined concrete-filled steel tubular columns under axial compression", *J. Compos. Constr.*, ASCE, **14**(1), 125-133.
- Dong, H.J. (2009), "Nonlinear analysis of the reinforced concrete member", MS thesis, *Dalian University of Technology*, Dalian China.
- Endo, K. and Unjo, S. (2005), "Analytical study on strength and ductility of long-span suspension bridge tower using concrete-filled steel tube", *J. Earthq. Eng.*, JSCE, **28**(31), 411-416.
- Endo, T., Shioi, Y., Hasegawa, A. and Wang, H.J. (2000), "Experimental study on reinforced concrete filled steel tubular structure", *Proc. 7th Int. Conf. on Steel Structures*, Singapore.
- Fan, X. and Zhou, G.Zh. (1998), "Experimental measure and computation about strain hardening modulus", *Journal of Tianjin Institute of Technology*, **14**(1), 1-4.
- Han, J.S., Xu, Z.D., Cong, S.P. et al. (2010), "Analysis of axial compressive performance for reinforced concrete filled tubular steel", *Arch. Environ. Eng.*, **31**(3), 11-17.
- Hu, H.T., Huang, C.S., Wu, M.H., and Wu, Y.M. (2003), "Nonlinear analysis of axially loaded concrete-filled tube columns with confinement effect", *J. Struct. Eng.*, ASCE, **129**(10), 1322-1329.
- Huang, C. S., et al. (2002), "Axial load behavior of stiffened concrete filled steel columns", *J. Struct. Eng.*, ASCE, **128**(9), 1222-1230.
- Jiang, X.M. (2007), "Study on mechanical performance and temperature field of concrete filled steel tubular short columns under axial compression", MS thesis, *Shandong University*, Jinan China.
- Jing, L.H., Xia, Z.F. and Hong, Sh.T. (2004), "Constitutive relations for concrete and its application", *Struct. Eng.*, **20**(6), 20-24.
- JSCE (2008), "Standard specifications for steel and composite structures - 2008 (IV seismic design)", *Japanese Society of Civil Engineers*, Tokyo Japan.
- JSCE (2007), "Standard specifications for concrete structures - 2007 (design)", *Japanese Society of Civil Engineers*, Tokyo Japan.
- JSCE (1999), "Reality state and analysis of steel construction damaged by Hanshin-Awaji Earthquake", *Japanese Society of Civil Engineers*, Tokyo Japan.
- JSCE (1999), "Theory and design of steel-concrete hybrid structures part1: Theory and basic concept", *Japanese Society of Civil Engineers*, Tokyo Japan.
- Lakshmi, B. and Shanmugam, N.E. (2002). "Nonlinear analysis of in-filled steel-concrete composite columns", *J. Struct. Eng.*, ASCE, **128**(7), 922-933
- Miao, W. (2010), "Experimental research and bearing capacity analysis of axially compressive reinforced concrete filled steel tube short column", *Shanxi Architecture*, **36**(5), 79-81.
- Mander, J. B., Priestley, M. J. N., and Park, R. (1988), "Theoretical stress-strain model for confined concrete", *J. Struct. Eng.*, ASCE, **114**(8), 1804-1826.
- Metin, H. and Selim, P. (2007), "Investigation of stress-strain models for confined high strength concrete", *Sadhana*, **32**(3), 243-252.
- Nishida, H. and Unjo, S. (2007), "Engineering discussions on allowable ductility factor of RC piers based on specifications for highway bridges of Japan", *Proc. 10th Symposium on Seismic Design of Bridges and Structures Based on the Ultimate Earthquake Resistance Method*, Tokyo Japan.
- Richart, F.E., Brandtzaeg, A., and Brown, R.L. (1928), "A study of the failure of concrete under combined compressive stresses", *Bull. 185, Univ. of Illinois Engineering Experimental Station*, Champaign, Ill.
- Sato, M. (2008), "Study on structural characteristics of RCFT and the application to practical structures", MS thesis, *Hachinohe Institute of Technology*, Hachinohe Japan.
- Shioi, Y. (1998), "Study on arrangement of reinforcements to improve shearing capacity and ductility of piers", *Report of study of science research subsidy*, Tokyo Japan.
- Su, X.D. (2007), "Nonlinear computer simulation for the reinforced concrete structure", MS thesis, *Southwest Jiaotong University*, Chengdu China.
- Suzuki, T. (2008), "Study on new bridges that adopt hybrid structure", PhD thesis, *Hachinohe Institute of*

- Technology*, Hachinohe Japan.
- Tadahiko, I. and Mokoto K. (2001), "Discussion of columns and beams using nonlinear analysis", *Prestressed Concrete*, **40**(2), 77-83.
- Wang, H.J., Ishibashi, H., Wei, H. and Hasegawa, A. (2002), "Experimental study on twin-column RCFT pier", the Second *Int. Conf. on Advances in Structural Engineering and Mechanics(ASEM'02)*, Busan(Pusan) Korea.
- Wei, H., Iwasaki, S., Hasegawa, A., Shioi, Y. and Miyamoto, Y. (2002), "Experimental study on mechanical characteristics of reinforced concrete filled circular steel tubular structures", *J. Constr. Steel*, JSSC, **10**, 519-526.
- Wei, H., Wang, H.J., Hasegawa, A. and Shioi, Y. (2005), "Study on strength of reinforced concrete filled circular steel tubular columns", *Struct. Eng. Mech.*, **19**(6), 653-677.
- Wu, M.H. (2000), "Numerical analysis of concrete filled steel tubes subjected to axial force". MS thesis, *Department of Civil Engineering, National Cheng Kung University, Tainan Taiwan R.O.C.*
- Xiao, C.Z., Cai, S.H. and Xu, C.L. (2005), "Experimental study on shear resistance performance of concrete filled steel tube columns", *China Civil Engineering Journal*, **12**(4), 10-16.
- Xu, Y. (2000), "Study on mechanical performance of rectangular concrete filled steel tubes structures", PhD thesis, *Tungchi University, Shanghai China.*
- Xu, Y.F., Zhao, J.Y., Liu, N. et al. (2009), "The ductility analysis of circular steel tube compile column filled with steel reinforced concrete on cyclic loading", *Journal of Shenyang Jianzhu University*, **10**(9), 83-87.
- Yao, G.H., Huang, Y.J., Song, B.D. et al. (2008), "Research on behavior of the inner joint of concrete filled steel tube column-RC ring beam", *Steel Constr.*, **9**(6), 27-30.
- Zhao, D.Z. (2003), "Study on the mechanical properties of steel tubular columns filled with steel-reinforced high-strength concrete", PhD thesis, *Dalian University of Technology, Dalian China.*
- Zhang, X.D. and Du D.N. (2006), "Application of ADINA in nonlinear analysis of reinforced concrete structure", *Science Technology and Engineering*, **14**(5), 78-81.